Dynamic modifications of polarizability for large metallic spheroidal nanoshells

H. Y. Chung (鍾弘毅),[1,2] P. T. Leung (梁培德),[1,a)] and D. P. Tsai (蔡定平)[1,2,3]
[1]*Department of Physics, National Taiwan University, Taipei 10617, Taiwan, Republic of China*
[2]*Instrument Technology Research Center, National Applied Research Laboratory, Hsinchu, Taiwan 300, Republic of China*
[3]*Research Center for Applied Sciences, Academia Sinica, Taipei 11529, Taiwan, Republic of China*

(Received 20 July 2009; accepted 2 September 2009; published online 29 September 2009)

We present an approach alternative to the hybridization model for the treatment of the coupled interfacial plasmon modes in spheroidal metallic nanoshells. Rather than formulating the problem from the Lagrangian dynamics of the free electronic fluid, we adopt an effective medium approach together with the uniqueness of the solutions to electromagnetic boundary value problem, from which the polarizability of the shells can then be systematically and efficiently derived; and the resonance frequencies for the coupled modes can be obtained from the poles in the polarizability. This approach can treat confocal nanoshells with different geometries for the spheroidal cavity and external surface and allow for a natural extension to incorporate corrections from the finiteness of the optical wavelength which are important for nanoparticles of larger sizes. This thus surpasses the hybridization model which is limited to incorporate only the electrostatic Coulomb interaction between the uncoupled plasmons. Numerical results will be provided for different nanoshell systems, and for the illustration of the various geometric and dynamic effects from our model.
 [doi:10.1063/1.3236528]

I. INTRODUCTION

Of the many plasmonic systems, metallic nanoparticles have become a very promising and versatile one for their great flexibility in many applications such as in various spectroscopy enhancement[1] and in the fabrication of nanoplasmonic waveguides.[2] As is well known, the plasmonic properties of these particles are largely determined by their geometry and the dielectric response of their materials. Among various geometries like bowtie, pyramidal, spherical, etc., the concentric shell geometry emerged as one with great potential for the large tunability in the plasmon modes of these nanoshells.[3]

First fabricated in 1998,[4] the metallic nanoshells evolved from spherical geometry to spheroidal geometry in the form of the "nanorice"[5] with even greater tunability and field enhancement in various applications. As is well known, while the field enhancement depends largely on the aspect ratio of the outside dimensions of the shell particle, the tunability arises from the coupling of the interfacial plasmon modes at both the outside and inside (i.e., cavity mode) surfaces of the particle. To theoretically describe both these properties in the long-wavelength limit, one has to calculate the polarizability and the coupled resonance frequencies of the particle. These, while rather straightforward to be obtained from solving the electrostatic boundary value problem for a spherical nanoshell, the problem will become rather nontrivial and complicated for more general geometries such as spheroidal shells.

In the last several years, a very useful theoretical scheme known as the "hybridization model (HM)" has been introduced for the treatment of the plasmonic response of such a system of concentric/confocal shells.[6–8] This HM is mainly built on the Lagrangian dynamics of the free electrons on the shell interfaces with the electrons described as a perfect fluid, and coupling between the electrons on different interfaces is accounted for from the static Coulomb interaction between these electrons. Coupled differential equations of motion for these interfacial electronic fluids are then derived in terms of their intrinsic (i.e., isolated) surface resonance frequencies, which upon solving yield the eigenfrequencies of the split (coupled) modes (e.g., the antibonding and bonding states) in exact agreement with the results obtained from solving the electrostatic boundary value problem. While the HM is powerful in that it can treat (i) shells with general spheroidal geometry,[8] (ii) structures with unlimited number of concentric shells ("nanomatryushka"[6,7]), and (iii) resonances of higher multipoles, it is strictly limited to the static response of the nanoshell and a generalization to incorporate dynamical effects in the optical response of these shells is not obvious and straightforward. Furthermore, while the HM can yield the coupled resonance frequencies rather systematically, the calculation of the polarizability itself from an eigenfunction solution of the HM can be quite involved. Because of this latter limitation, the optical absorption and extinction properties of these nanoshells have been occasionally calculated in an all-numerical approach (e.g., using methods such as FDTD, etc.).[6–8]

[a)]Author to whom correspondence should be addressed. Also affiliated with Institute of Optoelectronic Sciences, National Taiwan Ocean University, Keelung, Taiwan, ROC and Department of Physics, Portland State University, P. O. Box 751 Portland, Oregon 97207-0751, USA.

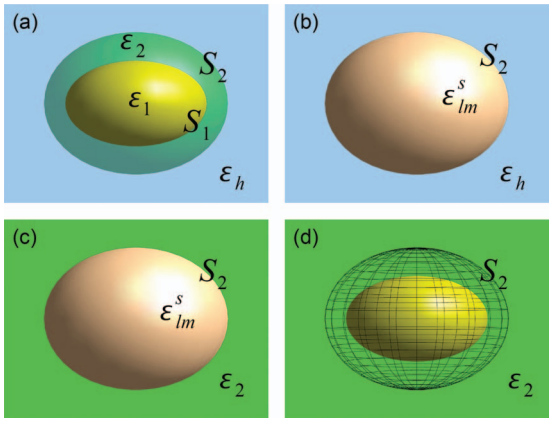

FIG. 1. Illustration of the approach of the LSC model, see text.

It is the purpose of this work to present an alternative approach to HM for the description of the optical response of these spheroidal nanoshells via their coupled plasmon modes. Our model is based on a generalization of the self-consistent effective medium model previously published by Li, Sun, and Chan (LSC) (Ref. 9) for spherical shells to spheroidal geometry, with the inclusion of the lowest order correction from the finiteness of the optical wavelength accounting for both the dynamic polarization and the radiative loss terms in the spirit of the so-called modified long wavelength approximation (MLWA).[10] While these latter dynamical effects have been formulated very recently for a spheroidal solid particle,[11] the corresponding results for spheroidal nanoshells have not yet been derived. Furthermore, just like the HM, our model can treat an unlimited number of concentric shells with *different* spheroidal geometries for the internal (cavity) and external surfaces. In addition, the polarizability of the nanoshells can be obtained more efficiently and from the poles of this quantity the coupled plasmonic resonance frequencies can be deduced. We shall first present the formulation of our theoretical model in the next section and follow with numerical results to illustrate the various geometric and dynamic effects for various nanoshell systems.

II. THEORETICAL MODEL

For definitiveness, we shall derive the multipolar polarizability α_{lm} of a single-layer spheroidal shell (in a host medium of dielectric constant ε_h) consisting of a core of dielectric function ε_1 and a (metallic) shell of dielectric function ε_2, with confocal surfaces [Fig. 1(a)]. Note that our effective medium approach below allows us (i) to avoid having to solve the complete boundary value problem which can be very complicated for spheroidal systems with a large number of concentric surfaces, (ii) to treat a multisurface system (e.g., the nanomatryushka) with two surfaces at a time, and (iii) to introduce the lowest order dynamic corrections to the electrostatic response in a systematic way.

A. The generalized LSC model

Following the LSC approach,[9] our goal is to construct, for each multipole order (l,m), an equivalent *solid* spheroidal particle [Fig. 1(b)] with an "effective dielectric function ε^s_{lm}" and a surface morphology identical to that of the outer surface of the original shell (i.e., S_2), such that its polarizability α_{lm} is identical to that of the shell. The key features of the LSC model consist of the following three steps:

(i) Assuming such an "effective spheroidal particle" is found, then we consider the situation when it is hypothetically placed in a medium with a dielectric function ε_2 which is identical to that of the material of the shell [Fig. 1(c)]. For such a case, one can obtain the following expression for the static polarizability of the spheroidal particle from standard solution of the boundary value problem [see Appendix A]:

$$\alpha^s_{lm} = a^{2l+1} C_{lm} \frac{\varepsilon^s_{lm} - \varepsilon_2}{\varepsilon^s_{lm} A_{lm}(\xi_2) - \varepsilon_2 B_{lm}(\xi_2)}, \tag{1}$$

where ξ_2 and a are the spheroidal coordinate and the foci, and the coefficients C_{lm}, A_{lm}, and B_{lm} are expressed in terms of the associated Legendre functions (P^m_l and Q^m_l) [see Appendix A for details].

(ii) Next, we go back to the original spheroidal shell and consider the case when it is also placed in a medium of dielectric function ε_2 [Fig. 1(d)], rather than in the host medium ε_h. In such a case, it is obvious that the system will simply respond just like a "bare particle" with boundary S_1 and dielectric function ε_1. In a similar way as in (i), we then obtain the polarizability of the shell in this case as follows:

$$\alpha^1_{lm} = a^{2l+1} C_{lm} \frac{\varepsilon_1 - \varepsilon_2}{\varepsilon_1 A_{lm}(\xi_1) - \varepsilon_2 B_{lm}(\xi_1)}. \tag{2}$$

Now if the "effective particle" really represents the original shell, then Eqs. (1) and (2) must give us identical results when each of them is placed in the same medium of dielectric function ε_2. Hence by setting $\alpha^s_{lm} = \alpha^1_{lm}$, we can solve for ε^s_{lm} and obtain the following result:

$$\varepsilon^s_{lm} = \varepsilon_2 \frac{\varepsilon_1[A_{lm}(\xi_1) - B_{lm}(\xi_2)] - \varepsilon_2[B_{lm}(\xi_1) - B_{lm}(\xi_2)]}{\varepsilon_1[A_{lm}(\xi_1) - A_{lm}(\xi_2)] - \varepsilon_2[B_{lm}(\xi_1) - A_{lm}(\xi_2)]}. \tag{3}$$

Note that although Eq. (3) is only a *necessary* condition that the dielectric function ε^s_{lm} of the effective particle must fulfill, the uniqueness in the boundary value problem solutions also guarantees it to be a sufficient condition. Hence, Eq. (3) implies that once the dielectric and geometric parameters of the original spheroidal shell are given, the effective ε^s_{lm} can be uniquely determined.

(iii) With the original spheroidal shell now replaced by a solid particle with an effective ε^s_{lm} in the same host medium (dielectric constant ε_h), the multipole polarizability of the original shell can then be obtained in the following form [cf. Eq. (1) or Eq. (2)]:

$$\alpha_{lm} = a^{2l+1} C_{lm} \frac{\varepsilon_{lm}^{s} - \varepsilon_h}{\varepsilon_{lm}^{s} A_{lm}(\xi_2) - \varepsilon_h B_{lm}(\xi_2)}$$
$$= a^{2l+1} C_{lm} \frac{(\varepsilon_2 - \varepsilon_h)[\varepsilon_1 A_{lm}(\xi_1) - \varepsilon_2 B_{lm}(\xi_1)] - (\varepsilon_1 - \varepsilon_2)[\varepsilon_2 B_{lm}(\xi_2) - \varepsilon_h A_{lm}(\xi_2)]}{[\varepsilon_1 A_{lm}(\xi_1) - \varepsilon_2 B_{lm}(\xi_1)][\varepsilon_2 A_{lm}(\xi_2) - \varepsilon_h B_{lm}(\xi_2)] - A_{lm}(\xi_2) B_{lm}(\xi_2)(\varepsilon_1 - \varepsilon_2)(\varepsilon_2 - \varepsilon_h)}. \quad (4)$$

If one adopts the ideal Drude model for the metallic shell: $\varepsilon_2(\omega) = \varepsilon_2' - \omega_p^2/\omega^2$, then the resonance frequency of order (l,m) can be obtained from the poles of Eq. (4) in the following form:

$$\omega_{lm}^{\pm} = \frac{\omega_p}{\sqrt{\varepsilon_2' - \varepsilon_{lm}^{\pm}}}, \quad (5)$$

with

$$\varepsilon_{lm}^{\pm} = \frac{1}{2p_{lm}}[-q_{lm} \pm \sqrt{q_{lm}^2 - 4p_{lm}r_{lm}}], \quad (6)$$

where

$$p_{lm} = A_{lm}(\xi_2)[B_{lm}(\xi_1) - B_{lm}(\xi_2)],$$

$$q_{lm} = \varepsilon_1 A_{lm}(\xi_2)[B_{lm}(\xi_2) - A_{lm}(\xi_1)] + \varepsilon_h B_{lm}(\xi_2)[A_{lm}(\xi_2) - B_{lm}(\xi_1)], \quad (7)$$

and

$$r_{lm} = \varepsilon_1 \varepsilon_h B_{lm}(\xi_2)[A_{lm}(\xi_1) - A_{lm}(\xi_2)].$$

B. Explicit results in the dipolar and spherical limits

We next give the explicit results for the dipolar response of a spheroidal shell and the general multipolar results in the limit of a spherical nanoshell:

(i) For dipolar response, we set $l=1$ in the above equations. Using the various results for the associated Legendre functions[12] to compute the various coefficients in Eq. (A11), we obtain the following results for the polarizability: for prolate spheroidal shells,

$$\alpha_{1m} = \frac{a^3}{3} \frac{(\varepsilon_2 - \varepsilon_h)(\varepsilon_1 F_1^m - \varepsilon_2 G_1^m) - (\varepsilon_1 - \varepsilon_2)(\varepsilon_2 G_2^m - \varepsilon_h F_2^m)}{(\varepsilon_1 F_1^m - \varepsilon_2 G_1^m)(\varepsilon_2 F_2^m - \varepsilon_h G_2^m) - (\varepsilon_1 - \varepsilon_2)(\varepsilon_2 - \varepsilon_h) F_2^m G_2^m}, \quad (8)$$

$$F_j^m = \frac{L_m(\xi_j)}{\xi_j(\xi_j^2 - 1)}, \quad G_j^m = \frac{L_m(\xi_j) - 1}{\xi_j(\xi_j^2 - 1)}, \quad j = 1 \text{ or } 2, \quad m = 0, \pm 1. \quad (9)$$

Here (L_0, L_1, L_{-1}) or equivalently (L_x, L_y, L_z) are the static geometrical factors which are defined as

$$L_0(\xi) = L_z(\xi) = (\xi^2 - 1)\left[\frac{\xi}{2}\ln\left(\frac{\xi+1}{\xi-1}\right) - 1\right],$$
$$L_{\pm 1}(\xi) = L_x(\xi) = L_y(\xi) = (1 - L_z(\xi))/2. \quad (10)$$

Note that these factors can also be expressed in a simple form in terms of the eccentricity of the spheroids.[11]

For oblate spheroidal shells,

$$\alpha_{1m}^{\text{oblate}}(\xi_1, \xi_2) = \alpha_{1m}^{\text{prolate}}(\xi_1 \to i\xi_1, \xi_2 \to i\xi_2). \quad (11)$$

Note that the Cartesian components can be obtained from the following relations:

$$\alpha_z = 4\pi\varepsilon_h \alpha_{10}, \quad \alpha_x = \alpha_y = 4\pi\varepsilon_h \alpha_{11}. \quad (12)$$

(ii) In the limit of a spherical shell, we consider the parameters $\xi_1 = r_1/a$, $\xi_2 = r_2/a$ (with $r_1 < r_2$) and then take the limit $a \to 0$ (hence $\xi_i \to \infty$). Since for $x \to \infty$, we have

$$P_l^m(x) \approx \frac{(2l-1)!!}{(l-m)!} i^{-m}(x)^l,$$
$$Q_l^m(x) \approx \frac{(l+m)!}{(2l+1)!!}(x)^{-l-1}, \quad (13)$$

we obtain for both the oblate and prolate spheroidal case:

$$A_{lm}(\xi) \approx C_{lm}\xi^{-2l-1}, \quad B_{lm}(\xi) \approx -\frac{l+1}{l} C_{lm}\xi^{-2l-1}. \quad (14)$$

Substituting Eq. (14) into Eq. (4) yields the following well-known result for a spherical shell:[13]

$$\alpha_{lm} = r_2^{2l+1} \frac{l(\varepsilon_2 - \varepsilon_h)[l\varepsilon_1 + (l+1)\varepsilon_2]r_2^{2l+1} + l(\varepsilon_1 - \varepsilon_2)[(l+1)\varepsilon_2 + l\varepsilon_h]r_1^{2l+1}}{[l\varepsilon_1 + (l+1)\varepsilon_2][l\varepsilon_2 + (l+1)\varepsilon_h]r_2^{2l+1} + l(l+1)(\varepsilon_1 - \varepsilon_2)(\varepsilon_2 - \varepsilon_h)r_1^{2l+1}}, \tag{15}$$

which is independent of m.

C. MLWA for spheroidal nanoshells

Next we discuss how the lowest order dynamic effects due to the finiteness of the optical wavelengths can be introduced into the above formalism in the spirit of the MLWA. Note that the MLWA is the *lowest* order correction, which applies only to the modification of the dipolar response [Eqs. (8)–(12) in Sec. II B above] and is consistent with the lowest order result from the exact Mie theory.[10,11] In spite of its limitations, the MLWA has been found to be quite accurate for the description of a large range of experiments on these nanoparticles.[14–18]

Note that, in the original formalism,[10] the MLWA was derived only for the case of a solid spherical particle. But since in the LSC model, a spherical shell is now replaced by an effective solid particle, the MLWA can thus be applied to shell structure as well, as has already been demonstrated in the original LSC paper.[9]

Hence, in order to formulate the MLWA for spheroidal shells, we first follow Moroz[11] to express the *static* dipolar (Rayleigh) polarizability of a spheroidal particle in a host (of dielectric constants ε and ε_h, respectively) as follows:

$$\alpha_{1m}^R = \frac{V}{4\pi} \frac{\varepsilon - \varepsilon_h}{\varepsilon_h + L_m(\varepsilon - \varepsilon_h)}, \tag{16}$$

where V is the volume of the particle, and the static geometrical factors L_m are as defined in Eq. (10). Next, as shown by Moroz,[11] the MLWA corrections of Meier and Wokaun[10] can be obtained for a spheroid by generalizing Eq. (16) to the following form:

$$\alpha_{1m}^{\mathrm{MW}} = \frac{\alpha_{1m}^R}{1 - (D_m/l_E)k^2\alpha_{1m}^R - i(2/3)k^3\alpha_{1m}^R} = \frac{V}{4\pi} \frac{\varepsilon - \varepsilon_h}{\varepsilon_h + q_m(\varepsilon - \varepsilon_h)}, \tag{17}$$

where l_E is the half length of the spheroidal axis along which the electric field is applied, and the generalized depolarizing factor q_m, which incorporates both geometric and dynamic effects, can be expressed as follows:

$$q_m = L_m - \frac{k^2 V}{4\pi l_E} D_m - i\frac{2k^3}{3}\frac{V}{4\pi}, \tag{18}$$

where D_m is the dynamic geometrical factor as given by Moroz,[11] and $k = 2\pi/\lambda$ is the wave vector in free space. Note that while the first term in Eq. (18) corresponds to the familiar static polarization term, the second and third terms give rise to the so-called dynamic polarization and radiation reaction which are originated from the exact electrodynamic fields of an oscillating dipole. Hence by using the appropriate quantities $L_m(\xi_j)$ and $q_m(\xi_j)$ with $j = 1, 2$ corresponding to the inner and outer shells, respectively, into the results expressed in Eqs. (8)–(12), we can obtain the MLWA results for the polarizability of a spheroidal nanoshell. We give more details for both spheroidal and spherical geometries as follows.

For prolate spheroidal shells (with $\xi \to i\xi$ for oblate case), the dynamic geometrical factors are given by[11]

$$D_0(\xi) = D_z(\xi) = \frac{3}{4}\left(\frac{\xi^2+1}{\xi^2-1}L_z(\xi) + 1\right),$$
$$D_{\pm 1}(\xi) = D_x(\xi) = \frac{\sqrt{\xi^2-1}}{2\xi}\left(3\xi \operatorname{arctanh}\left(\frac{1}{\xi}\right) - D_z(\xi)\right). \tag{19}$$

Hence the MLWA corrections can be obtained by simply replacing F_j^m and G_j^m in Eqs. (8) and (9) by the following expressions:

$$F_j^m \to \frac{q_m(\xi_j)}{\xi_j(\xi_j^2-1)}, \quad G_j^m \to \frac{q_m(\xi_j)-1}{\xi_j(\xi_j^2-1)},$$
$$j = 1 \text{ or } 2, \quad m = 0, \pm 1, \tag{20}$$

with q_m given in Eq. (18).

Although the above formalism is derived only for a single-layered nanoshell, it is rather straightforward to generalize it to a multilayered stratified system of spheroidal shells (a nanomatryushka) in a systematic way (see Appendix B).

Spherical limit. By setting $\xi_j = r_j/a$ and let $a \to 0$, we have

$$L_j \to \tfrac{1}{3}, \quad D_j \to 1, \quad \text{as } \xi \to \infty,$$
$$q_m(\xi_j) \to q_j = \tfrac{1}{3} - \tfrac{1}{3}x_j^2 - i\tfrac{2}{9}x_j^3, \tag{21}$$

where $x_j = kr_j = 2\pi r_j/\lambda$, and r_1 and r_2 are the radius of the inner and outer surfaces, respectively. In this limit, we have

$$F_j^m \to \frac{a^3}{r_j^3}q_j, \quad G_j^m \to \frac{a^3}{r_j^3}(q_j - 1),$$
$$j = 1 \text{ or } 2, \quad m = 0, \pm 1. \tag{22}$$

With the results in Eqs. (21) and (22), we finally obtain the following MLWA result for a spherical nanoshell:

$$\alpha_{1m} = \frac{1}{3} r_2^3 \frac{(\varepsilon_2 - \varepsilon_h)[\varepsilon_1 q_1 - \varepsilon_2(q_1 - 1)]r_2^3 - (\varepsilon_1 - \varepsilon_2)[\varepsilon_2(q_2 - 1) - \varepsilon_h q_2]r_1^3}{[\varepsilon_1 q_1 - \varepsilon_2(q_1 - 1)][\varepsilon_2 q_2 - \varepsilon_h(q_2 - 1)]r_2^3 - (\varepsilon_1 - \varepsilon_2)(\varepsilon_2 - \varepsilon_h)q_2(q_2 - 1)r_1^3}. \quad (23)$$

To our knowledge, the result in Eq. (23), being independent of m, has not been obtained before and is as significant as the corresponding one for spherical particles available in the literature.[14–18]

D. Improvements on MLWA

While the MLWA provides a simple recipe to include the lowest order dynamic corrections to the static polarizability for spheroidal nanoshells as illustrated above, the assumption of uniform polarization inside the particle renders the approach inaccurate for larger size particles. Following Stevenson[19] and Moroz,[11] we further introduce a semiempirical "improved MLWA" (IMLWA) which allows the particle polarization along the spheroidal axis of symmetry to vary in magnitude with the angle of inclination (θ) from this axis in the following form:

$$\vec{P} \to (1 + \beta k^2 r^2 \sin^2 \theta)\vec{P}, \quad (24)$$

where β is a dimensionless fitting parameter. As a consequence, following Moroz,[11] we obtain below a modified dynamic geometrical factor in place of the D_z in Eq. (19):

$$D_z = \frac{3}{4\pi a^2}[(1 - 2\beta)I_0 + (1 + 8\beta)I_1 - 6\beta I_2], \quad (25)$$

where the integrals over the particle volume are defined as

$$I_n = \int \frac{\cos^{2n}\theta}{2r} dV. \quad (26)$$

For a general spheroidal particle, the integrals in Eq. (26) are given in Ref. 11. For the simple case of a spherical particle, we have $I_n = \pi a^2/(2n+1)$ and $D_z \equiv D = 1 - (2/5)\beta$. In the following numerical studies, we shall also use this modified dynamic polarization as given in Eqs. (25) and (26) to illustrate how good the original MLWA can be improved to, in comparison with the exact electrodynamic results.

III. NUMERICAL RESULTS

In order to demonstrate the dynamical effects from our MLWA and IMLWA models formulated above for the optical response of a spheroidal nanoshell, we carried out some numerical studies on the coupled plasmon frequencies and the extinction cross sections of the silver nanoshell systems studied in Ref. 8 within the context of the HM. The dielectric function for silver as given in Ref. 8 has the following form: $\varepsilon(\omega) = \varepsilon_S - \omega_B^2/\omega(\omega + i\delta)$ with $\varepsilon_S = 5.0$, $\omega_B = 9.5$ eV, and $\delta = 0.15$ eV. To access the accuracy of our various long wavelength approximations, we first compared them with the exact electrodynamic results (Mie theory) for a spherical shell system which are easily available.[13] Figure 2 shows the calculation of the spectrum of the extinction cross section ($\sigma_{\text{ext}} = k \text{ Im } \alpha_1$) for a hollow silver spherical shell ($r_1 = 60$ nm and $r_2 = 70$ nm) according to all the three approximations (static, MLWA, and IMLWA with $\beta = 1$) in comparison with the exact electrodynamic result from the Mie theory.[13] As is clear from the figure, while the exact result shows both the split-dipole and the quadrupole modes, all the three approximations can only show the split-dipole modes as expected. Furthermore, while all of them give quite close results for the frequency ω_+ of the antibonding mode, significant errors occur in ω_- with the static model yielding blueshifted resonances, and the long-wavelength approximations leading to redshifted resonances for the bonding modes. Note that it is a rather general result that for a *hollow* shell, the high frequency ω_+ is relatively insensitive to the change in the interaction between the two individual plasmons, and thus retardation effects are quite insignificant for this mode. This is analogous to the in-phase oscillation of two coupled mechanical oscillators with characteristic frequencies quite insensitive to the strength of the coupling. Note also that the blueshifted peaks from static calculation also occur in a very general way, since retardation effect will lead to an overall weaker interaction between the cavity and the surface plasmons. Most importantly, one sees the significant failure of the static approximation for such a size of the shell (predicting in this case a blueshift of ~20% for ω_- and a peak approximately five times larger in value), and how the MLWA (and especially the IMLWA) can yield rather accurate results in comparison with the exact Mie theory. This thus confirms the usefulness of the MLWA in the calculation of dipole extinction for nanoshells of these dimensions which are often encountered in experimental studies, and are not too small compared to the optical wavelengths used in the experiments.

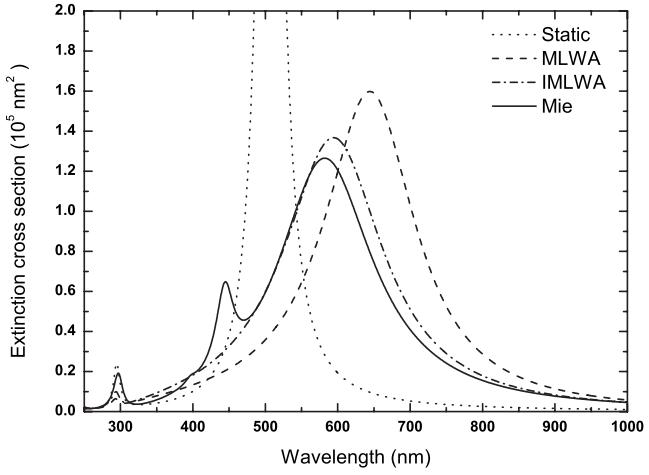

FIG. 2. Comparison of the extinction cross sections obtained in the static limit, from MLWA, and from IMLWA against the exact Mie theory results. The results are shown for a spherical nanoshell with inner radius of 60 nm and outer radius of 70 nm. The silver nanoshell is hollow inside and placed in vacuum.

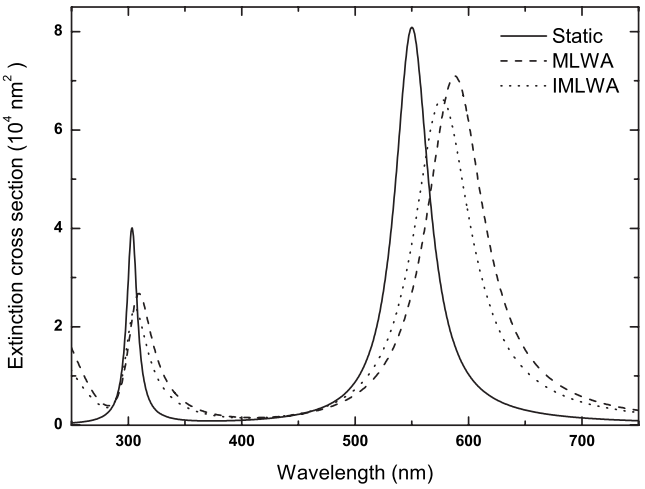

FIG. 3. Comparison of the extinction cross sections obtained in the static limit, from MLWA, and from IMLWA. The results are shown for a confocal prolate metallic shell with 40 nm foci and aspect ratios 1/2 (core) and 2/3 (outer surface). The nanoshell has a hematite core (ε=9.5) with the silver shell embedded in vacuum. The electric field is along the rotational symmetry axis of the spheroidal nanoshell.

Having established the accuracy of the MLWA for spherical nanoshells, we next apply them to the study of spheroidal shells. Figure 3 shows the calculation of the extinction cross section for the prolate silver spheroidal shell studied in Ref. 8 with a dielectric core (ε=9.5) and foci a=40 nm according to the three models: static, MLWA, and IMLWA. The complete geometry of the nanoshell is specified in the figure caption and the incident plane wave is polarized along the axis of rotational symmetry (note that our above formalism for the IMLWA only applies to this type of polarization). We notice that in this case the high frequency modes are still relatively insensitive to the different models. While the static results compare closely to those given by the HM (Ref. 20) (see Fig. 7 in Ref. 8), the significance of the corrections from both the long wavelength models is clearly revealed and is qualitatively similar to that found in the case for spherical shells. Again, we expect the result from IMLWA to be closer to the exact one from electrodynamics.

Having demonstrated the significance of the MLWA, we next apply it to study the effect of different aspect ratios on the extinction of the nanoshell. Figure 4 shows the MLWA results for the spheroidal nanoshell in Fig. 3 except that now the inner aspect ratio is varied. The polarization of the incident field is along [m=0, Fig. 4(a)] and perpendicular [m=1, Fig. 4(b)] to the rotational axis, respectively. For the m=0 case, one sees similar qualitative features for the resonance frequencies as observed in the static HM calculation[8] such as the redshifted bonding mode, and the almost-unchanged antibonding mode with the increase of the inner aspect ratio with fixed outer ratio. However, the values for the cross section obtained in our MLWA are quite different from those obtained in the HM as expected. For the m=1 case, Fig. 4(b) shows a stronger extinction for the antibonding mode, and the greater dependence of this resonance frequency on the inner aspect ratio, with a blueshifted peak as the ratio increases. For clarity, we have not shown the IMWLA results in Fig. 4(a) but we expect these results will give less redshifted resonances, and slightly lower peak cross sections compared with those obtained from the MWLA as shown.

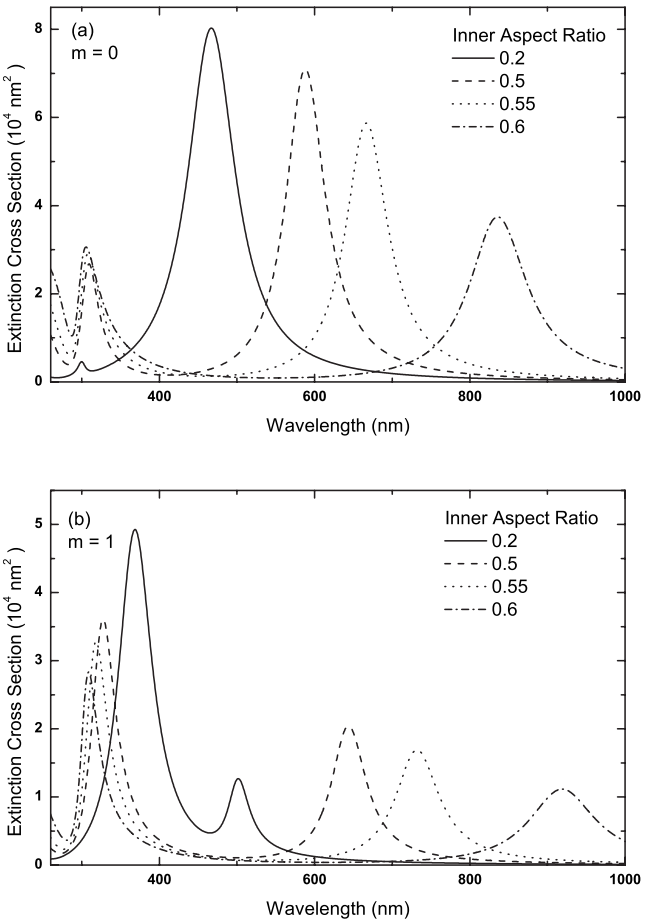

FIG. 4. The extinction cross sections of the confocal prolate metallic nanoshells (foci is fixed at 40 nm) with a fixed aspect ratio (2/3) for the outer surface and four different aspect ratios (0.2, 0.5, 0.55, and 0.6) for the core. The nanoshell has a hematite core (ε=9.5) with the silver shell embedded in the vacuum. The electric fields are oriented parallel (a) and perpendicular (b) to the rotational symmetry axis of the spheroidal nanoshell. The calculation is based on the MLWA model.

Finally, we also study the split eigenfrequencies using our model. Figure 5 shows the resonance frequencies of the coupled bonding and antibonding modes according to the three different models for the same spheroidal shell studied in Fig. 5 of Ref. 8. We show both the resonance wavelengths [Fig. 5(a)] and frequencies in eV [Fig. 5(b)] as a function of the inner aspect ratio of the shell. First we point out that our results according to the static model reproduce identical results as obtained from the HM [compare the solid curves in Fig. 5(b) to those in Fig. 5(c) in Ref. 8]. Those obtained from the MLWA, however, will give redshifted resonance frequencies in general. These redshifts are particular significant for the bonding modes in the present m=0 case; we also found (not shown) that they actually become more pronounced for the antibonding modes in the m=1 case for this filled shell (core with ε=9.5). In addition, we note that the dynamic modifications are more significant for lower inner aspect ratio of the shell as expected, since the effective scattering volume is greater in this case, which leads to a manifestation of the corrections from the finiteness of the wavelengths within the MLWA approach.

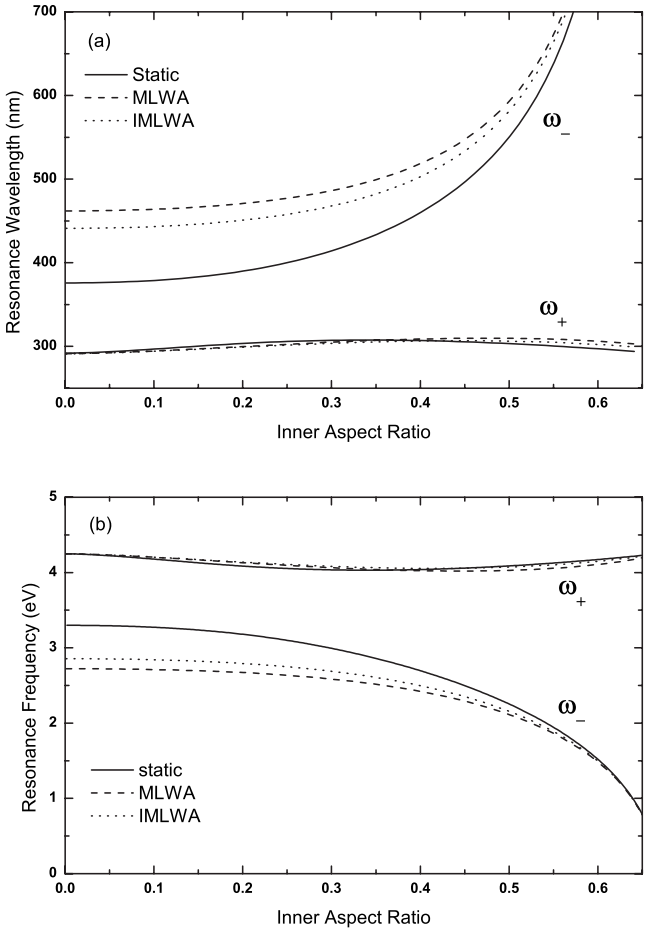

FIG. 5. Coupled resonance modes of a confocal prolate metallic nanoshell as a function of the aspect ratio of the core obtained from the static, MLWA, and IMLWA models, respectively. The aspect ratio of the outer surface and foci are fixed at 2/3 and 40 nm, respectively. The nanoshell has a hematite core ($\varepsilon=9.5$) with the silver shell embedded in the vacuum. The electric field is along the rotational symmetry axis of the spheroidal nanoshell. Note that (a) is in nanometers and (b) in eV for direct comparison with the results in Ref. 8.

IV. DISCUSSION AND CONCLUSION

In this work, we presented a systematic formulation, alternative to the HM, for the calculation of the polarizability and coupled resonance frequencies of a spheroidal metallic nanoshell (i.e., nanorice). Our effective medium approach generalizes the previous work (LSC, Ref. 9) to the spheroidal geometry, which allows for a very efficient computation of the polarizability of the nanoshells, as well as the incorporation of the lowest order dynamic effects in the framework of the MLWA (or IMLWA) for the description of the optical properties of these nanoparticles.

On the other hand, while the hybridization approach is powerful in many aspects in the account of the plasmonic coupling within these nanoshells including the physical origin of the split bonding and antibonding modes, the treatment of very general geometry of interacting surfaces such as two *external* spherical surfaces, two nonconcentric surfaces, etc., it will be rather nontrivial for it to go beyond the strictly static formulation based on the Coulomb interaction between the uncoupled plasmons, and to account for effects due to the finiteness of the optical wavelengths used in various spectroscopy experiments.

In a wide range of optical experiments involving these metallic nanoshells, it is likely that there is no need for a complicated full electrodynamic analysis of the observations due to the small sizes of these particles in comparison with the wavelengths. Moreover, recent studies reaffirmed that, the introduction of the lowest order dynamic effects in the form of the MLWA does provide a very good account for many of these experiments, in both far field[14–17] and near field[18] studies. Thus our present work of extending this MLWA (and IMLWA) to spheroidal metallic nanoshells should be of value for future understanding of various optical experiments with these systems of particles of not-too-small sizes (say, for 10 nm$<r<$100 nm), especially that our formulation not only yields the coupled resonance frequencies, but also the modified polarizability in a rather straightforward and systematic way. Thus it will be of interest and value to pursue further our present approach, to see if it can also handle other more irregular geometries (e.g., nonconcentric shells) so that it can really be established as a viable alternative to the HM for the description of the optical response of these irregular metallic nanoparticles.

ACKNOWLEDGMENTS

The authors are grateful for the research support from the National Science Council of Taiwan, R.O.C., under Project Nos. NSC-97-2120-M-002-013, NSC-96-2923-M-002-002-MY3, and NSC 97-2811-M-002-018, respectively, and to National Taiwan University and National Center for Theoretical Sciences, Taipei Office. P.T.L. would like to thank the additional support from a Fulbright Scholarship

APPENDIX A: STATIC POLARIZABILITY OF A SOLID SPHEROIDAL PARTICLE

To be self-contained, we here provide a brief account for the spheroidal coordinate system and for the multipole polarizability of a solid spheroidal particle.[21]

(i) The definition of spheroidal coordinates (ξ,η,φ).[12,21] Let us divide into the following two cases:

(a) Oblate spheroidal coordinates. Let a be the radius of the ring of foci with the ring lying on the xy plane, define

$$\xi=\sqrt{\left(\frac{\rho_1+\rho_2}{2a}\right)^2-1},\quad \eta=\pm\sqrt{1-\left(\frac{\rho_1-\rho_2}{2a}\right)^2},\tag{A1}$$

$$\varphi=\arctan\left(\frac{y}{x}\right);$$

with

$$\rho_1=\sqrt{(x+a\cos\varphi)^2+(y+a\sin\varphi)^2+z^2},$$
$$\rho_2=\sqrt{(x-a\cos\varphi)^2+(y-a\sin\varphi)^2+z^2}.\tag{A2}$$

Here ρ_1 and ρ_2 are the distances of the point (x,y,z) to the points of intersection of the ring of foci with the

plane through (x,y,z) and the z axis. The positive and negative sign of η correspond to $z>0$ and $z<0$, respectively.

(b) Prolate spheroidal coordinates. Let the two foci in this case be $(0,0,a)$ and $(0,0,-a)$ in Cartesian coordinates, respectively, and define

$$\xi=\frac{\rho_1+\rho_2}{2a},\quad \eta=\frac{\rho_1-\rho_2}{2a},\quad \varphi=\arctan\left(\frac{y}{x}\right), \tag{A3}$$

with

$$\rho_1=\sqrt{x^2+y^2+(z+a)^2},\quad \rho_2=\sqrt{x^2+y^2+(z-a)^2}. \tag{A4}$$

Here ρ_1 and ρ_2 are the distance of the point (x,y,z) to the two foci.

(ii) Polarizability of a solid spheroid.[21] Let us expand the electrostatic potential both inside and outside the spheroid (with boundary surface at $\xi=\xi_1$) as follows:

$$\psi_{\text{in}}(\xi,\eta,\varphi)=\sum_{l,m} c_{lm}X_l^m(\xi,a)Y_l^m(\cos^{-1}\ \eta,\varphi),$$

$$\psi_{\text{out}}(\xi,\eta,\varphi)=\sum_{l,m}[a_{lm}Z_l^m(\xi,a)+b_{lm}X_l^m(\xi,a)]Y_l^m(\cos^{-1}\ \eta,\varphi). \tag{A5}$$

For oblate spheroid we have

$$X_l^m(\xi,a)=i^{m-l}\frac{(l-m)!}{(2l-1)!!}a^lP_l^m(i\xi),$$

$$Z_l^m(\xi,a)=i^{l+1}\frac{(2l+1)!!}{(l+m)!}a^{-l-1}Q_l^m(i\xi), \tag{A6}$$

and for prolate spheroid,

$$X_l^m(\xi,a)=i^m\frac{(l-m)!}{(2l-1)!!}a^lP_l^m(\xi),$$

$$Z_l^m(\xi,a)=\frac{(2l+1)!!}{(l+m)!}a^{-l-1}Q_l^m(\xi). \tag{A7}$$

Here Y_l^m are the spherical harmonics, with $P_l^m(\xi)$ and $Q_l^m(\xi)$ as the associated Legendre functions of the first and second kind, respectively.

Applying the boundary conditions at the surface,

$$\psi_{\text{in}}(\xi,\eta,\varphi)|_{\xi=\xi_1}=\psi_{\text{out}}(\xi,\eta,\varphi)|_{\xi=\xi_1},$$

$$\varepsilon_1\left.\frac{\partial\psi_{\text{in}}(\xi,\eta,\varphi)}{\partial\xi}\right|_{\xi=\xi_1}=\varepsilon_2\left.\frac{\partial\psi_{\text{out}}(\xi,\eta,\varphi)}{\partial\xi}\right|_{\xi=\xi_1}, \tag{A8}$$

with ε_1 and ε_2 as the dielectric constant of the inside and the outside of the spheroid, respectively; a relation between a_{lm} and b_{lm} can be obtained:

$$a_{lm}=-(\varepsilon_2-\varepsilon_1)\left[\varepsilon_2\left.\frac{\partial Z_l^m(\xi,a)/\partial\xi}{\partial X_l^m(\xi,a)/\partial\xi}\right|_{\xi=\xi_1}-\varepsilon_1\frac{Z_l^m(\xi_1,a)}{X_l^m(\xi_1,a)}\right]^{-1}b_{lm}$$
$$\equiv-\alpha_{lm}b_{lm}. \tag{A9}$$

Thus the polarizability of the order of (l,m) can be obtained in this case as

$$\alpha_{lm}=a^{2l+1}C_{lm}\frac{\varepsilon_1-\varepsilon_2}{\varepsilon_1A_{lm}(\xi_1)-\varepsilon_2B_{lm}(\xi_1)},\quad \alpha_{lm}=\alpha_{l,-m}, \tag{A10}$$

where for oblate spheroid we have

$$A_{lm}(\xi)=\frac{Q_{lm}(i\xi)}{P_{lm}(i\xi)},\quad B_{lm}(\xi)=\frac{Q'_{lm}(i\xi)}{P'_{lm}(i\xi)},$$

$$C_{lm}=(-1)^{l+m}i^{-m-1}\frac{(l-m)!\,(l+m)!}{(2l-1)!\,!\,(2l+1)!\,!}, \tag{A11}$$

and for prolate spheroid,

$$A_{lm}(\xi)=\frac{Q_{lm}(\xi)}{P_{lm}(\xi)},\quad B_{lm}(\xi)=\frac{Q'_{lm}(\xi)}{P'_{lm}(\xi)},$$

$$C_{lm}=i^m\frac{(l-m)!\,(l+m)!}{(2l-1)!\,!\,(2l+1)!\,!}. \tag{A12}$$

APPENDIX B: RESULTS FOR A MULTILAYERED SPHEROIDAL "NANOMATRYUSHKA"

For a multilayered system of confocal spheroidal nanoshells, the LSC model can be applied to two of the shell surfaces at a time starting with the innermost two surfaces. For a system of n-layered shell, the following recurrence relation can be established by generalizing the result in Eq. (4):

$$\alpha_{lm}^n=a^{2l+1}C_{lm}\frac{(\varepsilon_n-\varepsilon_h)(\varepsilon_h\zeta_{lm}^{n-1}A_{lm}^{n-1}-\varepsilon_n\eta_{lm}^{n-1}B_{lm}^{n-1})-(\varepsilon_h\zeta_{lm}^{n-1}-\varepsilon_n\eta_{lm}^{n-1})(\varepsilon_nB_{lm}^n-\varepsilon_hA_{lm}^n)}{(\varepsilon_nA_{lm}^n-\varepsilon_hB_{lm}^n)(\varepsilon_h\zeta_{lm}^{n-1}A_{lm}^{n-1}-\varepsilon_n\eta_{lm}^{n-1}B_{lm}^{n-1})-A_{lm}^nB_{lm}^n(\varepsilon_h\zeta_{lm}^{n-1}-\varepsilon_n\eta_{lm}^{n-1})(\varepsilon_n-\varepsilon_h)}, \tag{B1}$$

where we define

$$A_{lm}^{n} = A_{lm}(\xi_n), \quad B_{lm}^{n} = B_{lm}(\xi_n), \quad \eta_{lm}^{n} = A_{lm}^{n}\alpha_{lm}^{n} - C_{lm}a^{2l+1},$$
$$\zeta_{lm}^{n} = B_{lm}^{n}\alpha_{lm}^{n} - C_{lm}a^{2l+1}, \tag{B2}$$

and the result in Eq. (4) is now the value for α_{lm}^{2}. Starting with this recurrence relation, one can then follow similar steps as described in Secs. II B and II C to obtain the MLWA for the dipolar polarizability of such a multilayered system.

[1] See, e.g., P. K. Jain, X. Huang, I. H. El-Sayed, and M. A. El-Sayed, "Review of some interesting surface plasmon resonance-enhanced properties of noble metal nanoparticles and their applications to biosystems" in the special issue of Plasmonics **2**, 107 (2007).
[2] For a recent review, see, e.g., S. A. Maier and H. A. Atwater, J. Appl. Phys. **98**, 011101 (2005).
[3] For recent reviews, see, e.g., L. R. Hirsch, A. M. Gobin, A. R. Lowery, F. Tam, R. A. Drezek, N. J. Halas, and J. L. West, Ann. Biomed. Eng. **34**, 15 (2006); S. Lal, N. K. Grady, J. Kundu, C. S. Levin, J. Britt Lassiter, and N. J. Halas, Chem. Soc. Rev. **37**, 898 (2008).
[4] S. J. Oldenburg, R. D. Averitt, S. L. Westcott, and N. J. Halas, Chem. Phys. Lett. **288**, 243 (1998).
[5] H. Wang, D. W. Brandl, F. Le, P. Nordlander, and N. J. Halas, Nano Lett. **6**, 827 (2006).
[6] E. Prodan, C. Radloff, N. J. Halas, and P. Nordlander, Science **302**, 419 (2003).
[7] E. Prodan and P. Nordlander, J. Chem. Phys. **120**, 5444 (2004); see also J. M. Steele, N. K. Grady, P. Nordlander, and N. J. Halas, Springer Ser. Opt. Sci. **131**, 183 (2007).
[8] D. W. Brandl and P. Nordlander, J. Chem. Phys. **126**, 144708 (2007).
[9] J. Li, G. Sun, and C. T. Chan, Phys. Rev. B **73**, 075117 (2006).
[10] M. Meier and A. Wokaun, Opt. Lett. **8**, 581 (1983).
[11] A. Moroz, J. Opt. Soc. Am. B **26**, 517 (2009).
[12] P. M. Morse and H. Feshbach, *Methods of Theoretical Physics, I and II* (McGraw-Hill, New York, 1953).
[13] C. F. Bohren and D. R. Huffman, *Absorption and Scattering of Light by Small Particles* (Wiley, New York, 1983).
[14] E. J. Zeman and G. C. Schatz, J. Phys. Chem. **91**, 634 (1987).
[15] W. H. Yang, G. C. Schatz, and R. P. van Duyne, J. Chem. Phys. **103**, 869 (1995).
[16] K. L. Kelly, E. Coronado, L. L. Zhao, and G. C. Schatz, J. Phys. Chem. B **107**, 668 (2003).
[17] B. T. Draine and P. J. Flatau, J. Opt. Soc. Am. A Opt. Image Sci. Vis. **11**, 1491 (1994).
[18] H. Mertens, A. F. Koenderink, and A. Polman, Phys. Rev. B **76**, 115123 (2007).
[19] A. F. Stevenson, J. Appl. Phys. **24**, 1134 (1953); **24**, 1143 (1953).
[20] Note that our extinction curves obtained in Fig. 3 are slightly narrower than those shown in Fig. 7 of Ref. 8, and the peak for the ω_+ mode is ~40% lower. We believe the discrepancy could have been caused by the different approach in the calculation of the dipole moments associated with the hybridized palsmon modes in Ref. 8.
[21] D. Bedeaux and J. Vlieger, *Optical Properties of Surfaces*, 2nd ed. (Imperial, London, 2004).